

Properties of Mn- and Co-doped bulk ZnO crystals

A. Y. Polyakov, N. B. Smirnov, A. V. Govorkov, and E. A. Kozhukhova
Institute of Rare Metals, Moscow, 119017, B. Tolmachevsky, 5, Russia

Y. W. Heo, M. P. Ivill, K. Ip, D. P. Norton, and S. J. Pearton^{a)}
Department of Materials Science and Engineering, University of Florida, Gainesville, Florida 32611

J. Kelly, R. Rairigh, and A. F. Hebard
Department of Physics, University of Florida, Gainesville, Florida 32611

T. Steiner
Air Force Office of Scientific Research, Arlington, Virginia 22217

(Received 29 October 2004; accepted 13 December 2004; published 21 January 2005)

Electrical and magnetic properties, room temperature optical absorption bands, and 300 and 90 K microcathodo luminescence (MCL) bands were studied in heavily Mn and Co doped (1–5 at. %) bulk ZnO crystals. Optical absorption bands near 1.9 eV (Co) and 2 eV (Mn) and MCL bands near 1.84 eV (Co) and 1.89 eV (Mn) are found to be associated with transition metal (TM) ions. These bands are assigned to internal transitions between the levels of the substitutional TM ions. The temperature dependence of the resistivity of the ZnO showed activation energies of ~ 35 meV in all cases and the electron mobilities were decreased relative to the undoped material. © 2005 American Vacuum Society. [DOI: 10.1116/1.1856476]

I. INTRODUCTION

ZnO continues to attract attention for short wavelength emission, transparent electronics, and spintronic devices because of its large exciton binding energy, ability to be grown at low temperatures on cheap substrates, and the ability to achieve room temperature ferromagnetism by doping with transition metals.^{1–22} The model by Dietl *et al.*^{23,24} predicts that the transition temperature in diluted magnetic semiconductors (DMS) will scale with a reduction in the atomic mass of the constituent elements due to an increase in p - d hybridization and a reduction in spin-orbit coupling and suggests that a T_c greater than 300 K is possible for p -type ZnO. Ferromagnetism in magnetically doped ZnO has also been theoretically investigated by *ab initio* calculations based on local density approximation.^{25,26} For V, Cr, Fe, Co, and Ni dopants, ferromagnetic ordering in ZnO is predicted to occur without the need of additional charge carriers. The properties of transition metal (TM) impurities are of particular interest due to the predicted room temperature ferromagnetism of heavily TM doped ZnO.

TM dopants can be incorporated into ZnO both during growth (from vapor phase, by solid state recrystallization, by hydrothermal method, or, e.g., from PbF₂ solutions) or through direct ion implantation.^{27–36} The most thoroughly studied system is Fe-doped ZnO.³⁷ Electron spin resonance (ESR) of these samples showed clear indications of the presence of the Fe³⁺ ionized donors in semi-insulating material with the Fermi level deep in the band gap.³⁷ The signal was photosensitive and could be quenched by light with photon energies peaked near 2.75 eV which was explained by optically stimulated transition from Fe³⁺ to Fe²⁺ state by capturing

an electron from the valence band. Detailed studies placed the optical ionization transition threshold from the Fe³⁺ state to the conduction band at about 1.4 eV indicating a strong lattice coupling of the deep donor state of Fe in ZnO.³⁷ A similar photosensitive ESR signal was observed for Ni doped ZnO,³⁷ while ESR signals in the Mn- and Co-doped ZnO were found not to be photosensitive. For the Co-doped material a strong optical band at 0.55–0.66 μm was detected in absorption and photocurrent spectra and attributed to an optical transition from the ground state to the excited states of the Co ion with subsequent thermal excitation of the electrons into the conduction band.³⁷ The electrical properties of Mn and Co were studied by means of current-voltage (I - V), capacitance-voltage (C - V) and isothermal capacitance transients (ICTS) in ZnO crystals solution grown from PbF₂.³⁸ No indication of the presence of deep states that could be related to Mn and Co were observed in ICTS spectra which could point to respective centers being deeper than the Schottky barrier height (~ 0.7 eV).

In this article we report on the electrical, magnetic, and optical properties of Mn- and Co-doped bulk ZnO grown by the hydrothermal method.

II. EXPERIMENT

The magnetic properties were obtained using a commercially available rf-superconducting quantum interference device (Quantum Design MPMS). None of the films showed any evidence of second phase formation from x-ray diffraction measurements. The room temperature optical transmission spectra were obtained using a Hitachi 330 spectrophotometer. These were complemented by microcathodo luminescence (MCL) spectra measurements at 90 and 300 K. The electron concentrations and mobilities of the samples were characterized by standard van der Pauw measurements

^{a)}Author to whom correspondence should be addressed; electronic mail: spear@mse.ufl.edu

TABLE I. Electrical measurements on ZnO crystals.

(a) ZnO control sample				
Temperature, K	ρ , Ω cm	μ , $\text{cm}^2/\text{V s}$	N , cm^{-3}	E_a , eV
293	0.385	222	7.3×10^{16}	0.035
77	1.02	1350	1.55×10^{15}	
(b) ZnO(1% Mn) sample				
Temperature, K	ρ , Ω cm	μ , $\text{cm}^2/\text{V s}$	N , cm^{-3}	E_a , eV
293	9.8×10^{-2}	160	4.1×10^{17}	0.025
77	0.855	316	2.4×10^{16}	
(c) ZnO(5% Mn) sample				
Temperature, K	ρ , Ω cm	μ , $\text{cm}^2/\text{V s}$	N , cm^{-3}	E_a , eV
293	0.174	27.5	1.3×10^{18}	0.030
77	3.28	42.5	4.5×10^{16}	
(d) ZnO(1% Co) sample				
Temperature, K	ρ , Ω cm	μ , $\text{cm}^2/\text{V s}$	N , cm^{-3}	E_a , eV
293	4.93×10^{-2}	136	9.3×10^{17}	0.032
77	0.746	317	2.6×10^{16}	

at 77 and 300 K with In ohmic contact. Schottky diodes were prepared by Ag evaporation through a shadow mask (diodes' diameter close to 1 mm) on substrates that were not specially heated. Sample preparation included cleaning in organic solvents, blowing dry with nitrogen, short (10 s) etching in concentrated hot (40 °C) HCl, rinse in de-ionized water, blowing dry. In this case the ohmic contacts were made by attaching silver paste to the backside of the samples. On all samples we measured optical transmission spectra using an Hitachi 330 UV-visible spectrophotometer. MCL spectra were taken at 300 and 90 K with various excitation intensities to elucidate the nature of the observed bands. On samples with Schottky diodes capacitance-voltage (C - V), capacitance versus frequency (C - f), capacitance/conductance versus temperature (C / G - T), deep level transient spectroscopy (DLTS) measurements were carried out C - V , C - f , and C / G - T experiments were performed at frequencies from 10 Hz to 10 MHz in the temperature range 85–400 K, using a HP 4192 low frequency impedance analyzer deep level transient spectroscopy (DLTS) measurements were performed either with electrical pulse injection or with optical pulse injection (ODLTS for brevity). In both cases the measurements were carried out using a HP4280A C - V / C - t meter with external pulse generator HP8112A. Optical injection was provided by illumination with a deuterium lamp source equipped with mechanical shutter actuated by the pulse generator.

III. RESULTS

Results of van der Pauw measurements are summarized in Table I. Undoped control samples had electron concentration of $7 \times 10^{16} \text{ cm}^{-3}$ and mobility of $222 \text{ cm}^2/\text{V s}$. The temperature dependence of conductivity showed the activation energy of the dominant donors as 35 meV. The carrier concentration was slightly higher with TM doping and the mobilities distinctly lower, but this appears to be the result of

introducing additional donors and possibly scattering on the high density of neutral centers. If the TM ions substitute the Zn they should act as deep donors and would be neutral in n -type material. The slopes observed in the temperature dependences of resistivity are probably consistent with the 35 meV donors attributed to hydrogen.⁴

Figure 1 (top) shows room temperature hysteresis present in the 1 at. % Mn-doped sample. The bottom of the figure

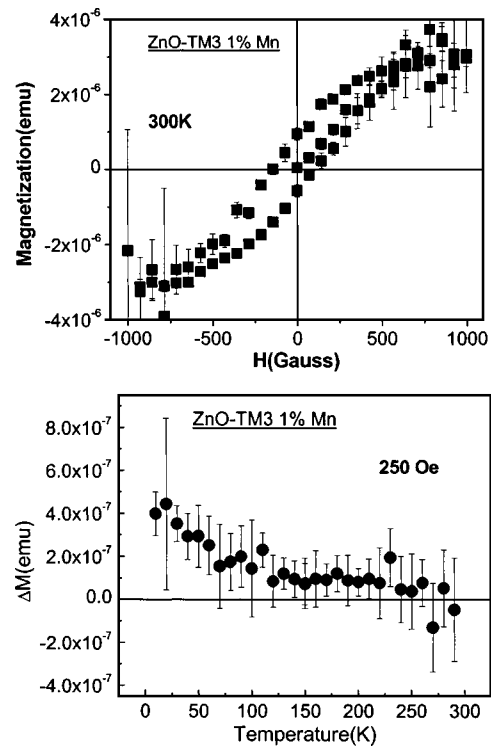


FIG. 1. Hysteresis loop (300 K) in bulk ZnO crystal doped with 1 at. % Mn (top), along with the difference in field-cooled and zero-field-cooled magnetization as a function of temperature (bottom).

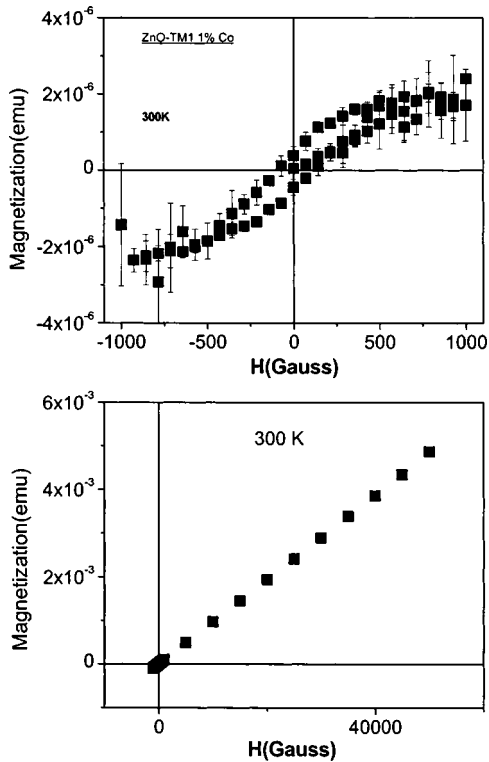


FIG. 2. Magnetization vs field at 300 K for bulk ZnO crystals doped with 1 at. % Co (top) or 5 at. % Mn (bottom).

shows the temperature dependence of the difference in magnetization, $\Delta M(T) = M_{FC}(T) - M_{ZFC}(T)$, between the field-cooled and the zero-field-cooled data. The difference between the two plots advantageously eliminates para- and diamagnetic contributions and indicates the presence of hysteresis if the difference is nonzero. Although ferromagnetism is the usual explanation for hysteresis, spin glass effects, cooperative interactions between superparamagnetic clusters, or superparamagnetism below a blocking temperature can also be the cause. All of these effects, however, are magnetic phenomena involving the ordering of spins, and it is in this sense that we refer to the hysteresis measured by the $\Delta M(T)$ data as “ferromagnetic.” The $\Delta M(T)$ plot of Fig. 1 has a strong positive curvature and approaches zero near room temperature. Identification of T_c from such a plot as the temperature at which $\Delta M(T)$ equals zero is at best a statement about the disappearance of hysteresis at the 250 Oe field in which the data are acquired. Similar data taken at lower fields will have a higher T_c . These rather unconventional shapes in the temperature-dependent magnetization were first seen in (Ga,Mn)As and are common in most diluted magnetic diluted magnetic semiconductor (DMS) materials. Explanations for this behavior can be found in theoretical treatments that consider the effect of randomness and disorder on percolating ferromagnetic clusters.^{27,28}

Figure 2 (top) shows that the 1 at. % Co-doped sample exhibited similar room temperature hysteresis, while the 5 at. % Mn-doped ZnO was paramagnetic (bottom). The lat-

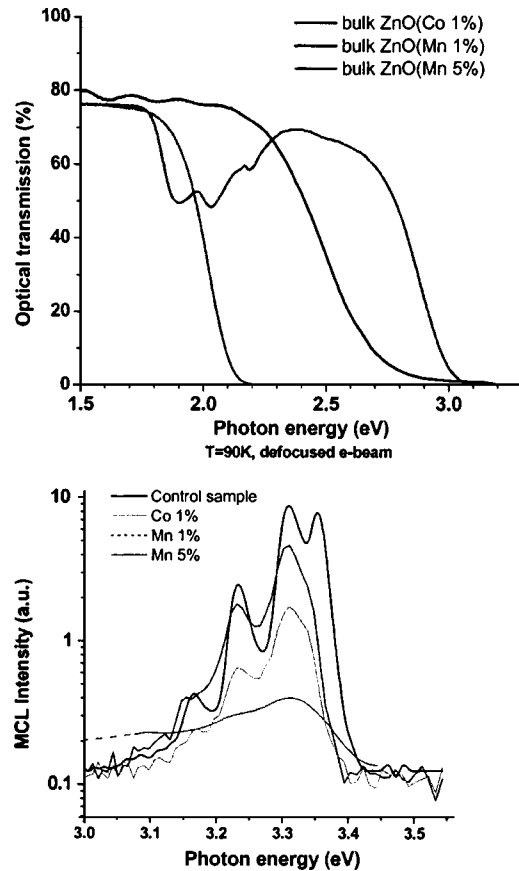


FIG. 3. Room temperature optical transmission spectra for the bulk ZnO samples (top) and near-band-edge MCL spectra taken on 90 K on the same samples (bottom).

ter result is consistent with theory in that over-doping increases the antiferromagnetic direct coupling between the Mn ions.

Optical transmission spectra of the TM-doped samples are shown at the top of Fig. 3. The ZnO (1% Co) shows a triplet which comes from the internal transitions and is expected for the Co^{2+} state split by the crystal field and a strong absorption band near 2.6 eV. It could be excitation from the deep donors due to the Co or to some defects that are introduced during growth. The ZnO (1% Mn) data correspond to absorption bands near 2 eV assigned to internal transitions between the levels of the substitutional Mn ions. Increasing the Mn concentration to 5% results in one strong absorption band near 1.8 eV. Figure 3 (top) shows a blowup of the excitonic region of the 90 K MCL spectra while the full spectra are shown in Fig. 4. The control sample shows the usual excitonic series in the UV and a weak defect band near 2.4 eV. In the TM-doped samples the intensity is greatly decreased (in fact, the measurements are taken with the e-beam current 170 times higher than for the undoped sample). The intensity of the first excitonic line near 3.35 eV is virtually zero, and the intensity of the other lines decreases as Mn 1%, Co, Mn 5%. There also appears a strong band near 2.2 eV and, for Co, a strong band near 1.8 eV. At room temperature one sees a strong decrease in the excitonic near-band-edge region, a

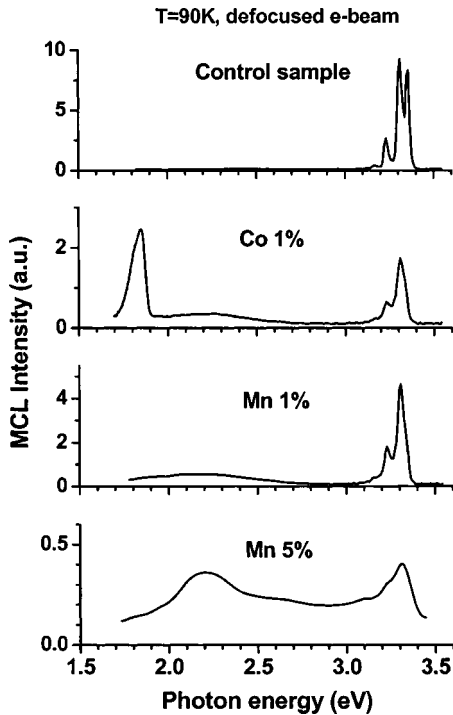


FIG. 4. 4 MCL spectra (90 K) from undoped bulk ZnO and the transition metal-doped samples.

strong increase of intensity near 2.2 eV and, for Co, a strong band near 1.8 eV. The optical transmission spectrum of the virgin ZnO crystal showed no strong absorption bands anywhere but at the band-edge region.

Figure 5 shows the current-voltage (I - V) characteristics of all diodes at room temperature. In the forward direction the ideality factor is 1.4 for the control sample and 2.5 for the 1 at. % Mn and Co-doped samples. In the case of the 5 at. % Mn-doped sample, we were not able to get any rectification on diodes prepared in the standard fashion.³⁸ However a brief (30 min) anneal in O_2 at 70 °C, followed by deposition of the Ag contact produced reasonable rectification in this sample. Our measurements show that this treatment created a resistive surface layer that decreased the total measured capacitance and the leakage current, even though the material underneath was still highly conducting (see below). One ex-

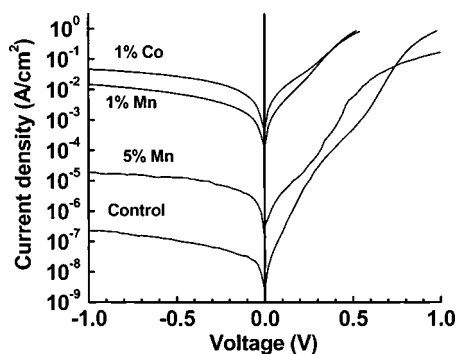


FIG. 5. Room temperature I - V characteristics of control, 1% Mn, 5% Mn, and 1% Co samples.

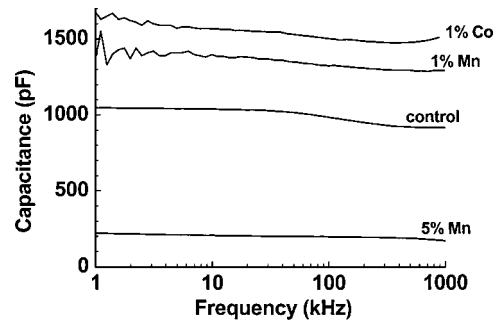


FIG. 6. Room temperature C - f characteristics of control, 1% Mn, 5% Mn, and 1% Co samples.

planation is that we have removed some hydrogen from the near-surface region when annealing in oxygen at 70 °C.³⁹ Annealing in oxygen can also change the stoichiometry and hence the resistivity, but that occurs only at higher annealing temperatures (close to 700 °C). The increase of the reverse current of the doped diodes correlates with the higher concentration of shallow donors deduced from Hall measurements (Table I). The temperature dependence of the current both in the forward and in reverse direction is very small and much less than expected from the barrier height measured from capacitance-voltage (C - V). This suggests that tunneling is the dominant transport mechanism. Although the electron concentration measured by Hall is much higher in the 5% Mn sample the reverse current is almost as low as for the control sample. The series resistance is even higher than in the control sample and the ideality factor is also higher (1.8 vs 1.4). This suggests that there is a less conducting layer at the surface of this sample.

Capacitance-frequency (C - f) characteristics measured at room temperature are shown in Fig. 6. The capacitance increases considerably from control sample to the doped samples as would be expected from the Hall data. The capacitance of the 5% Mn sample was the lowest, although the electron concentration in the bulk is the highest. C - V measurements at 100 kHz yielded a barrier height of ~ 0.8 eV and concentrations of uncompensated donors of $8 \times 10^{16} \text{ cm}^{-3}$ for the control sample, $5 \times 10^{17} \text{ cm}^{-3}$ for the 1% Mn sample and $9 \times 10^{17} \text{ cm}^{-3}$ for the 1% Co sample. These results correlate well with the Hall data.

Figure 7 shows the admittance spectra of the control sample. Two centers can be clearly seen. One has an activation energy of 0.33 eV and is also observed in DLTS (see below), the other is the center with the activation energy of 70 meV. Both centers were observed previously in ZnO that was proton implanted or exposed to hydrogen plasmas.^{37,40,41} The 0.3 eV centers are the dominant deep traps in undoped ZnO and have been reported by Auret *et al.*⁵ The other traps, the 70 meV centers, are not the sole shallow donors because the capacitance does not freeze out to zero at low temperatures (Fig. 7).

Figure 8 shows admittance spectra for the 1% Co sample. The leakage current was much higher than on the control sample and to make the peaks in conductance visible we

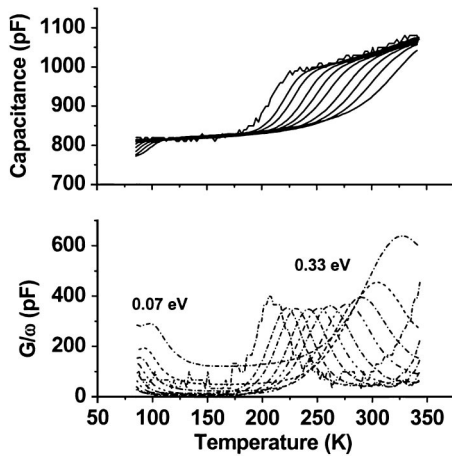


FIG. 7. C - T (upper graph) and G/ω - T (lower graph) curves measured at 300 Hz, and 1, 2, 5, 10, 20, 50, 100, 200, and 500 kHz for control sample.

subtracted the conductance at 1 kHz from the raw data. The 0.3 eV centers are still present, but the 70 meV donors are no longer observed. In the Mn-doped samples the 0.3 eV traps are also observed in admittance, but no 70 meV traps were present. If one also considers that the shallow donor concentration in the Mn, Co-doped samples increased considerably compared to the control sample and that the activation energy of the dominant centers is close to 35 meV and may be related to hydrogen.¹

In the deep level transient spectroscopy (DLTS) spectrum for the control sample, Fig. 9, we see one dominant trap with activation energy of 0.3 eV and concentration 10^{15} cm^{-3} . This is the same trap detected in admittance spectroscopy and the one reported to be the dominant trap in undoped n -ZnO⁵ (the $\Delta C/C$ signal was converted into concentration by multiplying it by $2N_d^*F$ (F is the spectrometer function: $1/[\exp(-t_2 \ln(t_2/t_1))/(t_2-t_1)] - \exp(-t_1 \ln(t_2/t_1))/(t_2-t_1)$]; for the peak it gives the concentration of the traps save for the λ correction, but this is small for all traps but the 0.9 eV hole trap). In the two doped samples the concentration of the 0.3 eV trap did not change much compared to the control

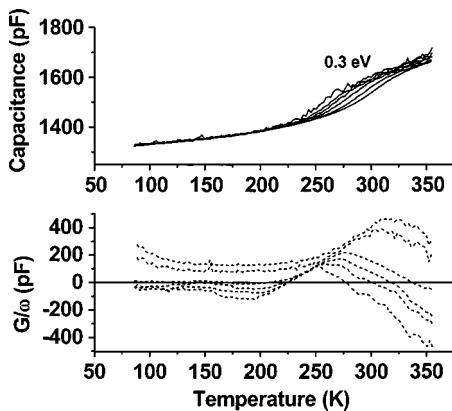


FIG. 8. C - T (upper graph) and G/ω - T (lower graph) curves measured at 10, 20, 30, 50, 100, and 200 kHz for the 1% Co sample (G/ω - T characteristics were obtained after subtracting the 1 kHz curve to correct for the higher leakage current).

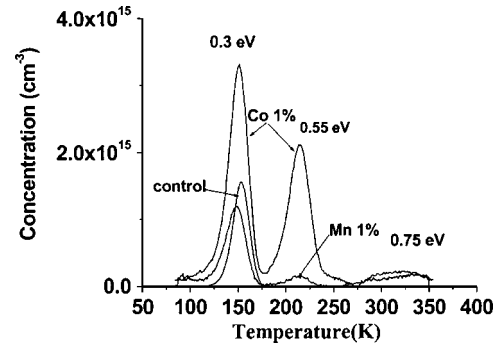


FIG. 9. DLTS spectra taken on control sample, 1% Mn sample, and 1% Co sample with reverse bias of -1 V, forward bias pulse of 1 V (100 ms long) and time windows of 100/1000 ms.

sample. We do observe two traps at 0.55 and 0.75 eV whose concentration is much higher in the 1% Co sample. These traps are very similar to the ones reported in proton implanted ZnO.^{4,40,41} The 0.55 eV traps were also reported in plasma treated ZnO samples.⁴¹ Their concentration (and the concentration of the 0.75 eV traps) increased with the TM concentration and they are believed to be structural defects.

With optical excitation (deuterium lamp) we see virtually no signal in the control sample (Fig. 10) and two hole traps at $E_V+0.2$ eV and $E_V+0.9$ eV in the doped samples. These traps have also been reported in proton-implanted ZnO⁴⁰ and thus are not specifically related to the transition metal ions.

IV. SUMMARY AND CONCLUSIONS

In summary, bulk Mn and Co-doped ZnO crystals show room temperature ferromagnetism for TM concentrations of ~ 1 at. %. At higher concentrations the films become paramagnetic due to direct coupling between the transition metal ions. This approach looks extremely promising as a foundation for future ZnO-based spintronic devices such as polarized UV light emitters and spin-field effect transistors.

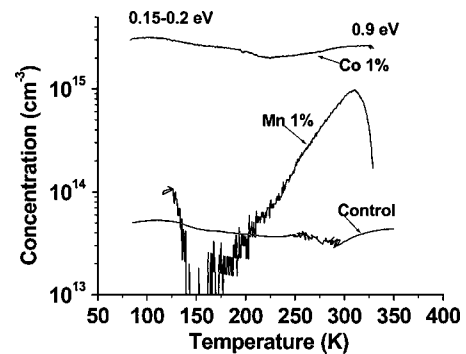


FIG. 10. ODLTS spectra taken on control sample, 1% Mn sample and 1% Co sample with reverse bias of -1 V, optical injection pulse of 2 s (UV deuterium lamp with mechanical shutter) and time windows of 100/1000 ms.

ACKNOWLEDGMENTS

The work at IRM was supported in part by the Russian Foundation for Basic Research (Grant No. 04-02-16510). The work at UF is partially supported by NSF (DMR 0400416), AFOSR F49620-03-1-0370 and ARO(DAAD-190210420). The authors would like to thank E. F. Astakhova and G. V. Shepekina for experimental assistance.

- ¹D. C. Look, *Mater. Sci. Eng.*, B **80**, 383 (2001).
- ²R. L. Hoffman, *J. Appl. Phys.* **95**, 5813 (2004).
- ³Y. Ohya, T. Niwa, T. Ban, and Y. Takahashi, *Jpn. J. Appl. Phys.*, Part 1 **40**, 297 (2001).
- ⁴Y. Kwon, Y. Li, Y. W. Heo, M. Jones, P. H. Holloway, D. P. Norton, Z. V. Park, and S. Li, *Appl. Phys. Lett.* **84**, 2685 (2004).
- ⁵F. D. Auret, S. A. Goodman, M. Hayes, M. J. Legodi, H. A. v. Laarhoven, and D. C. Look, *Appl. Phys. Lett.* **79**, 3074 (2001).
- ⁶S. Choojun, R. D. Vispute, W. Wang, R. P. Sharma, T. Venkatesan, and H. Shen, *Appl. Phys. Lett.* **80**, 1529 (2002).
- ⁷J. Narayan, A. K. Sharma, A. Kvit, C. Jin, J. F. Muth, and O. W. Holland, *Solid State Commun.* **121**, 9 (2002).
- ⁸Y. I. Alivov, E. V. Kalinina, A. E. Cherenkov, D. C. Look, B. M. Ataev, and A. K. Omaev, *Appl. Phys. Lett.* **83**, 4719 (2003).
- ⁹Y. I. Alivov, J. E. V. Nostrand, D. C. Look, and M. V. Chukichev, *Appl. Phys. Lett.* **83**, 2943 (2003).
- ¹⁰K. Sato and H. Katayama-Yoshida, *Jpn. J. Appl. Phys.*, Part 2 **39**, L555 (2000).
- ¹¹H.-J. Lee, S.-Y. Jeong, C. R. Cho, and C. H. Park, *Appl. Phys. Lett.* **81**, 4020 (2002).
- ¹²S.-J. Han, J. W. Song, C.-H. Yang, S. H. Park, J.-H. Park, Y. H. Jeong, and K. W. Rhie, *Appl. Phys. Lett.* **81**, 4212 (2002).
- ¹³S. W. Jung, S.-J. An, G.-C. Yi, C. U. Jung, S.-I. Lee, and S. Cho, *Appl. Phys. Lett.* **80**, 4561 (2002).
- ¹⁴T. Fukumura, Z. Jin, M. Kawasaki, T. Shono, T. Hasegawa, S. Koshihara, and H. Koinuma, *Appl. Phys. Lett.* **78**, 958 (2001).
- ¹⁵D. P. Norton, S. J. Pearton, A. F. Hebard, N. Theodoropoulou, L. A. Boatner, and R. G. Wilson, *Appl. Phys. Lett.* **82**, 239 (2003).
- ¹⁶M. S. Park and B. I. Min, *Phys. Rev. B* **68**, 224436 (2003).
- ¹⁷A. S. Risbud, N. A. Spaldin, Z. Q. Chen, S. Stemmer, and R. Seshadri, *Phys. Rev. B* **68**, 205202 (2003).
- ¹⁸S.-J. Han, T.-H. Jang, Y. B. Kim, B.-G. Park, J.-H. Park, and Y. H. Jeong, *Appl. Phys. Lett.* **83**, 920 (2003).
- ¹⁹S. W. Yoon, S.-B. Cho, S. C. We, S. Yoon, B. J. Suh, H. K. Song, and Y. J. Shin, *J. Appl. Phys.* **93**, 7879 (2003).
- ²⁰X. M. Cheng and C. L. Chien, *J. Appl. Phys.* **93**, 7876 (2003).
- ²¹S. S. Kim, J. H. Moon, B.-T. Lee, O. S. Song, and J. H. Je, *J. Appl. Phys.* **95**, 454 (2004).
- ²²S. Kolesnik, B. Dabrowski, and J. Mais, *J. Appl. Phys.* **95**, 2582 (2004).
- ²³T. Dietl, H. Ohno, F. Matsukura, J. Cibert, and D. Ferrand, *Science* **287**, 1019 (2000).
- ²⁴T. Dietl, *Semicond. Sci. Technol.* **17**, 377 (2002).
- ²⁵K. Sato and H. Katayama-Yoshida, *Jpn. J. Appl. Phys.*, Part 2 **39**, L555 (2000).
- ²⁶K. Sato and H. Katayama-Yoshida, *Semicond. Sci. Technol.* **17**, 367 (2002).
- ²⁷I. P. Kuz'mina and V. A. Nikitenko, *Zinc Oxide: Growth and Optical Properties* (Nauka, Moscow, 1984) (in Russian).
- ²⁸S.-J. Han, J. W. Song, C.-H. Yang, S. H. Park, J.-H. Park, J. H. Jeong, and K. W. Rhie, *Appl. Phys. Lett.* **81**, 4212 (2002).
- ²⁹N. Ohashi, J. Tanaka, T. Ohgaki, H. Haneda, M. Ozawa, and T. Tsurumi, *J. Mater. Res.* **17**, 1529 (2002).
- ³⁰D. P. Norton, S. J. Pearton, A. F. Hebard, N. Theodoropoulou, L. A. Boatner, and R. G. Wilson, *Appl. Phys. Lett.* **82**, 239 (2003).
- ³¹T. Fukumura, Z. Jin, A. Ohtomo, H. Koinuma, and M. Kawasaki, *Appl. Phys. Lett.* **78**, 958 (2001).
- ³²A. Tiwari, C. Jin, A. Kvit, D. Kumar, J. F. Muth, and J. Narayan, *Solid State Commun.* **121**, 371 (2002).
- ³³S.-J. Han, T. H. Jang, Y. B. Kim, B. G. Park, J. H. Park, and Y. H. Jeong, *Appl. Phys. Lett.* **83**, 920 (2003).
- ³⁴S. W. Jung, S.-J. An, G.-C. Yi, C. U. Jung, S.-I. Lee, and S. Cho, *Appl. Phys. Lett.* **80**, 4561 (2002).
- ³⁵P. Sharma, A. Gupta, K. V. Rao, F. J. Owens, R. Sharma, R. Ahuja, J. M. Osorio Guillen, B. Johansson, and G. A. Gehring, *Nat. Mater.* **2**, 673 (2003).
- ³⁶N. Theodoropoulou, G. P. Berera, V. Misra, P. LeCalir, J. Philip, J. S. Moodera, B. Satapi, and T. Som (to be published).
- ³⁷M. Berciu and R. N. Bhatt, *Phys. Rev. Lett.* **87**, 107203 (2001).
- ³⁸S. Das Sarma, E. H. Hwang, and A. Kaminski, *Phys. Rev. B* **67**, 155201 (2003).
- ³⁹C. H. Seager and S. M. Myers, *J. Appl. Phys.* **94**, 2888 (2003).
- ⁴⁰A. Polyakov, N. Smirnov, A. Govorkov, E. Kozhukhova, V. Vdovin, K. Ip, M. Overberg, Y. Heo, S. J. Pearton, D. Norton, J. M. Zavada, and V. Dravin, *J. Appl. Phys.* **94**, 2895 (2003).
- ⁴¹A. Y. Polyakov, N. B. Smirnov, A. Gorokov, K. Ip, M. E. Overberg, Y. Heo, D. P. Norton, S. J. Pearton, B. Luo, F. Ren, and J. M. Zavada, *J. Appl. Phys.* **94**, 400 (2003).